Published May 2007
Published online May 17, 2007

Special Section: Savannah River Site
Vadose Zone Journal

Monitoring Surface and Subsurface Water Storage Using Confined Aquifer Water Levels at the Savannah River Site, USA

Todd C. Rasmussen* and Thomas L. Mote

Surface and subsurface water storage is an important component of hydrologic models, needed to account for groundwater recharge, lateral water movement, and evapotranspiration. Yet methods for estimating above- and belowground water storage include substantial uncertainties. This paper demonstrates that water levels in the Gordon aquifer (a confined aquifer at the USDOE Savannah River Site, near Aiken, SC) fluctuate in response to changes in total water storage. An increase in surface loading is known to cause a measurable increase in aquifer fluid pressure whenever the aquifer skeletal compressibility is sufficiently large. Water levels in the Gordon aquifer respond rapidly during precipitation events, which is consistent with increased loading that compresses the aquifer at depth. Instantaneous barometric and loading efficiencies of approximately 6 and 91%, respectively, are consistent with a poorly consolidated aquifer. Because the aquifer has a high loading efficiency, it behaves like a geological weighing lysimeter that appears to estimate water storage. Following precipitation events, aquifer water levels decline over time, presumably due to unloading by evapotranspiration plus net lateral water export. The water-storage signal is improved by incorporating (i) the lagged response between aquifer load and borehole water-level changes and (ii) the removal of periodic Earth tides.

Water levels in wells that tap confined aquifers are widely observed to fluctuate in response to loads on the Earth's surface. Blaise Pascal (1973) noted the effects of barometric pressure changes on water levels in wells in 1663, and much later, C.E. Jacob (1940) noted the effects of trains on water levels in wells tapping confined aquifers. A potentially useful new application is the use of these observed changes in confined aquifer water levels to estimate above- and belowground water storage. The use of confined aquifers as geological weighing lysimeters was only recently proposed by van der Kamp at a site in southern Saskatchewan, Canada (van der Kamp and Maathuis, 1991; van der Kamp and Schmidt, 1997; Barr et al., 2000). This approach was subsequently confirmed at additional sites in Matamata, New Zealand (Bardsley and Campbell, 1994, 1995, 2000), northern New South Wales, Australia (Timms and Acworth, 2005), and western Kansas (Sophocleous et al., 2006).

A confined aquifer at the Savannah River Site, SC, also shows apparent responses to load changes. Water levels in observation wells within the Gordon aquifer (a poorly consolidated, confined, Coastal Plain aquifer) demonstrate large and rapid changes in response to aquifer loading. Specifically, we show that water levels rapidly increase in response to precipitation events, with subsequent slow declines that are attributed to evapotranspiration losses plus net lateral water movement.

We also show how regression deconvolution can be used to improve the loading signal. Regression deconvolution is used to account for the delay between the application of a load and the time when a water-level response is observed (Rasmussen and Crawford, 1997; Spane, 2002). The lagged response is attributed to the time required for borehole water levels to equilibrate with the total head in the monitored aquifer. The regression deconvolution response compares favorably with a slug test conducted in the same well. The regression deconvolution approach also removes the effect of Earth tides, which is a significant exogenous variable that also affects the aquifer load signal. The statistical approach provides better removal than when the theoretical Earth tide is used as the exogenous variable.

The geologic weighing lysimeter approach provides auxiliary information about surface and subsurface water storage, a critical component in ecosystem studies. The geologic weighing lysimeter is not suited to all sites, however. As discussed here, suitable geologic units include those with low barometric efficiencies (corresponding to high loading efficiencies), relatively

T.C. Rasmussen, Warnell School of Forestry and Natural Resources, The Univ. of Georgia, Athens, GA 30602-2152; T.L. Mote, Dep. of Geography, The Univ. of Georgia, Athens, GA 30602-2502. Received 24 Mar. 2006. *Corresponding author (trasmuss@uga.edu).

Vadose Zone J. 6:327–335
doi:10.2136/vzj2006.0049

stable flow conditions, and minimal natural or anthropogenic disruptions. Such disruptions are a function of the proximity of the site to recharge or pumping boundaries, and the hydraulic properties of the aquifer.

Theory

Aquifer Loading Theory

Water levels in wells commonly fluctuate in response to barometric pressure changes. Water-level changes in elastic, confined aquifers are usually some fraction of the barometric pressure change (Davis and Rasmussen, 1993; Rasmussen and Crawford, 1997):

$$\alpha = -\frac{\Delta W}{\Delta B} \quad [1]$$

where α is the barometric efficiency of the aquifer, $\triangle W$ is the change in borehole water level, and $\triangle B$ is the barometric pressure change. The total head in a borehole, H_b, is found by adding the observed water level, W, and the barometric pressure head, B (Spane and Mercer, 1985). Changes in borehole head over time, $\triangle H_b$, are similarly related to

$$\Delta H_b = \Delta W + \Delta B = (1-\alpha)\Delta B \quad [2]$$

The total head within a confined aquifer, H_a, responds to surface loading as a function of the elasticity of the aquifer skeleton. That is, the mineral skeleton of a poorly consolidated aquifer tends to bear only a small fraction of the surface load, L, causing an increase in the load borne by aquifer fluids (Jacob, 1940):

$$\Delta H_a = \beta \Delta L \quad [3]$$

where β is the loading efficiency. For the case in which the borehole head equals the aquifer head, $\triangle H_a = \triangle H_b$, and the barometric pressure is the cause of the increased load, $\triangle B = \triangle L$, then $\alpha + \beta = 1$.

When the load is also affected by overlying water storage changes, $\triangle S$, then

$$\Delta H_a = \beta (\Delta B + \Delta S) \quad [4]$$

For the case in which the borehole head equals the aquifer head, $\triangle H_a = \triangle H_b$, and the barometric pressure is known:

$$\Delta S = \frac{\Delta H_a}{\beta} - \Delta B = \frac{\Delta W + \Delta B}{\beta} - \Delta B \quad [5]$$

Changes in water storage are a function of precipitation inputs, P, and the water export, $\triangle R$:

$$\Delta S = P - \Delta R \quad [6]$$

Rearranging yields results in

$$\Delta R = P + \Delta B - \frac{\Delta W + \Delta B}{\beta} \quad [7]$$

The terms on the right-hand side of Eq. [7] can be monitored, yielding an independent estimate of the water export term. The water export term, $\triangle R = ET + Q$, is a function of two processes, net evapotranspiration, ET, and lateral fluxes, Q, which are more difficult to determine than other components of the water budget.

Loading Efficiency Estimation

For the above section, an important assumption was the equivalence between the aquifer head changes, $\triangle H_a$, and total head changes within the borehole, $\triangle H_b$. In general, however, there is likely to be a delay between these two, analogous to the effects of an aquifer slug test in which borehole water levels require a period of time to equilibrate with the total head within the aquifer. This delayed response can be attributed to a number of factors, including borehole storage, poor well construction, and dual porosity within the aquifer.

The lagged response can be found statistically using regression deconvolution (Furbish, 1991; Rasmussen and Crawford, 1997; Spane, 2002). This technique uses a unit response function, μ, to relate the observed time series of inputs, $\triangle L$, to the observed output time series (total head changes in the borehole, $\triangle H_b$):

$$\Delta H_b = \mu * \Delta L \quad [8]$$

where * is the convolution operator, defined using the convolution summation:

$$y(t) = h(\tau) * x(t) = \sum_{\tau=0}^{m} h(\tau) x(t-\tau) \quad [9]$$

where x is the input variable, y is the output variable, h is the unit response function, t is the time variable, τ is the lag variable, and m is the memory of the system. The response function approach is conceptually equivalent to the use of unit hydrographs in surface-water hydrology, in which regression deconvolution is used to obtain the unit hydrograph with precipitation as the input time series and stream discharge as the output time series (McCuen, 2004).

To apply this method for this problem, a set of equations are written in the form

$$\Delta H_b(t) = \mu(0)\Delta L(t) + \mu(1)\Delta L(t-1) + \ldots + \mu(m)\Delta L(t-m) \quad [10]$$

or

$$\Delta H_b(t) = \sum_{\tau=0}^{m} \mu(\tau)\Delta L(t-\tau) \quad [11]$$

where $\mu(\tau)$ is the unit response function for the load efficiency at lag τ.

For a specific data set, there will be a column vector of observed borehole head changes, $\triangle H_b(t)$, along with the matrix of observed load changes, $\triangle L(t - \tau)$, in which each column represents a lagged set of loads starting with an unlagged column on the left, with successive columns being lagged by one additional interval. Standard statistical or mathematical packages can be used to estimate the unit response function, $\mu(\tau)$, using ordinary least squares (McCuen, 2004).

The step response function is found using

$$\beta(\tau) = \sum_{i=0}^{\tau} \mu(i) \quad [12]$$

where τ is the response lag.

Because the regression analysis focuses on short-term changes (every 10 min for this application), the effects of evapotranspiration and lateral migration can be neglected. These processes are much slower, and the effects on differences can be readily neglected. Thus, the observed load changes can be represented using the sum of the interval precipitation plus barometric pressure changes: $\triangle L \approx P + \triangle B$.

In addition to finding the unit response function to changes in loads, the regression deconvolution algorithm can also be used to remove other exogenous variables. Water levels in wells are known to fluctuate in response to solar and lunar forces, collectively called Earth tides (Rojstaczer and Agnew, 1989). These fluctuations have a strongly sinusoidal behavior, with a complex mixture of diurnal (an approximate 24-h period) and semidiurnal (an approximate 12-h period) components (Melchior, 1983).

Earth-tide effects were removed using a finite sum of the principal solar and lunar tidal components that are likely to affect water-level fluctuations:

$$\varepsilon(t) = \sum_{i=1}^{n} \left(a_i \cos\omega_i t + b_i \sin\omega_i t \right) \quad [13]$$

where n is the total number of Earth-tide components, a_i and b_i are the regression-estimated magnitudes of these components, and the frequencies, $w_i = 2\pi/p_i$, correspond to the principal diurnal and semidiurnal tidal components with periods, p_i. The primary solar diurnal and semidiurnal cycles, S1 and S2 (corresponding to exactly 24 and 12 h), were not used because of the risk of removing the evapotranspiration signal, which contains these periods.

In this case, the right-hand side matrix of Eq. [11] is augmented with an additional 2 × n columns. Each pair of n columns corresponds to the cos $w_i t$ and sin $w_i t$ terms, respectively, and the n columns correspond to the n different w_i frequencies. The n pairs of linear coefficients, a_i and b_i, are estimated simultaneously with the unit response function using ordinary least squares regression. The delay-corrected water storage is then calculated using

$$\Delta S(t) = \frac{1}{\mu(0)} \left\{ \Delta H_b(t) - \varepsilon(t) - \sum_{i=1}^{m} \mu(i) \left[\Delta B(t-i) + \Delta S(t-i) \right] \right\} - \Delta B(t) \quad [14]$$

and the water export is calculated using

$$\Delta R(t) = P - \Delta S(t) \quad [15]$$

The water storage and cumulative export are the sum of these functions, $S = \Sigma\triangle S$ and $R = \Sigma\triangle R$.

Materials and Methods

Site Description

The Savannah River Site is a 790-km^2 area operated by the USDOE on the Atlantic Coastal Plain province in southwestern South Carolina near the Georgia–South Carolina border (Fig. 1). The FSB-120 well cluster is located at 33.27312°N and 81.68413°W on a broad ridge in the Sand Hill region. This region is characterized by a northeast-southwest trending series of flat hills with long, smooth side slopes in sandy and loamy

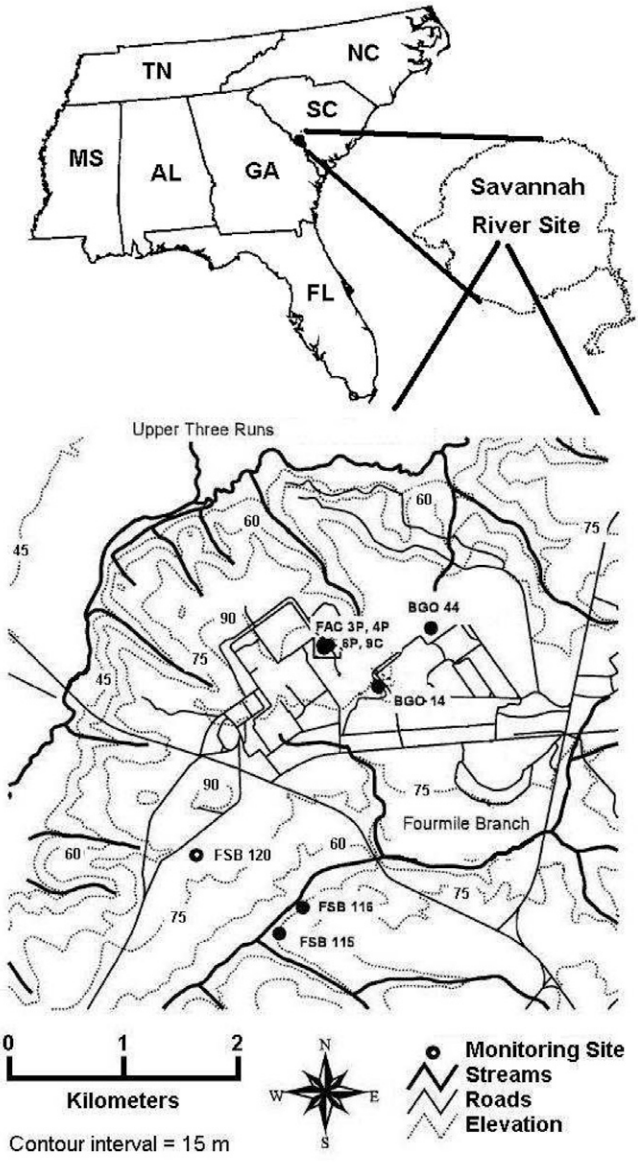

FIG. 1. Location map showing the Savannah River Site, SC, (top), and FSB-120 well cluster within the General Separations Area (bottom).

Coastal Plain sediments. Soils surrounding the well cluster are Troup Sands, which are well-drained, moderately permeable, loamy, siliceous, thermic Grossarenic Paleudults. The solum is generally greater than 1.5-m thick, with a sandy surface horizon and a loamy subsoil (Rogers, 1990). Below the solum is an unsaturated zone comprised primarily of loose sands, with a water table that lies approximately 20 m below the ground surface.

The climate at the site is warm (moist) temperate, with average annual high and low temperatures of 24.0 and 11.7°C, respectively. The average high temperature in the warmest month, July, is 32.8°C, and the average low temperature during the coldest month, January, is 1.4°C. The average annual precipitation is approximately 1214 mm, with no pronounced seasonal variation (Rogers, 1990). Despite the ample rainfall, overland flow is generally absent near the FSB-120 well cluster due to the coarse sandy soils and flat topography. The area is forested, primarily as planted pine plantations (*Pinus taeda* and *P. elliottii*). Streams run parallel to the ridge line of this sand hill; Upper

Three Runs is to the northwest, and Four-Mile Branch is to the southeast. These perennial streams flow toward the southwest and are sustained by groundwater inflows at or below seepage lines within the riparian zone.

The subsurface hydrology consists of a sequence of unconfined, semiconfined, and confined aquifers, shown in Fig. 2. Groundwater flow at the site is primarily vertical within the unsaturated zone and horizontal within the Floridan Aquifer System, which extends across the site and includes all strata from the water table to the top of confining beds in the Paleocene Black Mingo Group (Aadland et al., 1995). The uppermost aquifer is the Upper Three Runs aquifer, which consists of an unconfined (surficial) and a semiconfined (Barnwell-McBean) unit. Lateral groundwater movement through the unconfined and semiconfined aquifers are toward the southeast (136°), that is, toward Four-Mile Branch (Bruns, 2000). Below the semiconfined unit is the Gordon Confining Unit, informally called the Green Clay Interval, which consists of one or more thin but persistent clay beds. The Green Clay varies in thickness from 0.6 to 3 m and has a vertical hydraulic conductivity of approximately 5.5×10^{-3} cm per day.

The primary aquifer of concern in this study is the Gordon aquifer, which is the uppermost confined aquifer. The Gordon aquifer varies in thickness from 20 to 30 m, has a horizontal hydraulic conductivity of approximately 860 cm per day and a hydraulic diffusivity of 8.64×10^{-9} cm^2 per day (Rasmussen et al., 2003). The Meyers Branch Confining System separates the Gordon from the underlying Dublin aquifer. This confining system is approximately 12-m thick at the northwest boundary of the Savannah River Site but thickens to about 30 m near the southeast boundary. The unit has a vertical hydraulic conductivity of approximately 9.5×10^{-3} cm per day. Clay and silt beds make up most of the unit. The dark, fine-grained sediments represent lower delta plain, bay-dominated environments (Aadland, 1993).

Because the hydraulic conductivities of the confining units above and below the Gordon aquifer are five orders of magnitude less than the hydraulic conductivity of the Gordon aquifer, horizontal flow conditions predominate at the site. The poor hydraulic communication between the adjacent aquifers is also consistent with the observed long-term containment of chemical and nuclear contaminants within the overlying aquifers despite a vertical (downward) hydraulic gradient across the Green Clay greater than 1 (Bruns, 2000). While the Gordon aquifer is regionally extensive and an important water resource, local use is absent. The lack of human and natural perturbations to the aquifer within and near the Savannah River Site results in minimal water-level fluctuations.

Data Acquisition

Water levels within three aquifers at Well Cluster FSB-120 were monitored for 258 d between 29 Oct. 1994 and 14 July 1995. Well FSB-120D was used to monitor water levels in the uppermost (surficial) aquifer, FSB-120C in the Barnwell-McBean (semiconfined) aquifer, and FSB-120A in the Gordon (confined) aquifer. Monitored water levels included the target aquifer along with two overlying units. Well completion information is provided in Table 1.

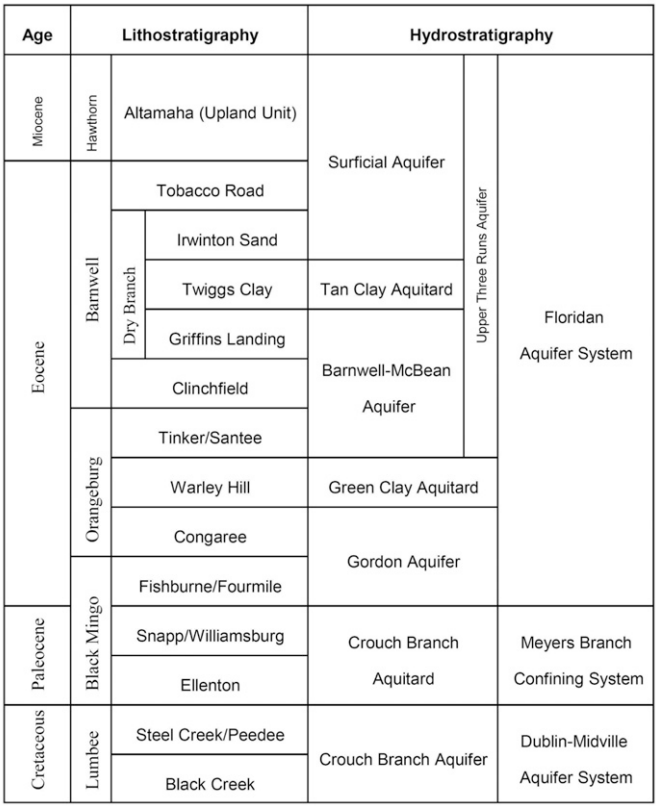

Fig. 2. Lithostratigraphic and hydrostratigraphic units at the Savannah River Site, SC.

Borehole water levels were monitored using Druck PDCR 830 series, 3.5-m gage-type pressure transducer (Druck, Inc., New Fairfield, CT) (accurate to 0.35 cm). Automated readings were checked against manual depth-to-water readings using a Powers Well Sounder (Powers Electric Product Co., Inc., Fresno, CA). Precipitation at the well cluster was monitored using a Rainwise tipping-bucket recording raingage (RainWise, Inc. Bar Harbor, ME) (accurate to 0.025 cm). Total precipitation was checked against a Tru-Chek manual raingage (Tru-Chek, Inc., Albert Lee, MN). Barometric pressure was monitored using a Vaisala PTB100A analog barometer (Vaisala, Inc., Boston MA) (accurate to 0.03 cm).

Peripheral devices were connected to a Campbell Scientific CR-10 datalogger (Campbell Scientific, Inc., Logan, UT). While all peripherals were monitored every second, the datalogger calculated and recorded total precipitation and average water levels and barometric pressures every 10 min. Measurement accuracy improved using averaged values instead of individual measure-

Table 1. FSB-120 water-level monitoring well cluster, Savannah River Site, SC.

	Monitoring well		
	FSB-120D	FSB-120C	FSB-120A
Aquifer type	Surficial	Semiconfined	Confined
UTM North (m)†	3 681 582.35	3 681 578.99	3 681 576.75
UTM East (m)†	436 287.04	436 292.61	436 295.39
Ground surface elevation (m)	84.9	84.7	84.8
Screen zone elevation, top (m)	66.0	49.0	33.2
Screen zone elevation, bottom (m)	59.9	45.9	30.2
Water level elevation (m)	63.1	62.5	45.2
Casing diameter (cm)	10	10	10
Casing type	PVC	PVC	PVC

†UTM, Universal Transverse Mercator.

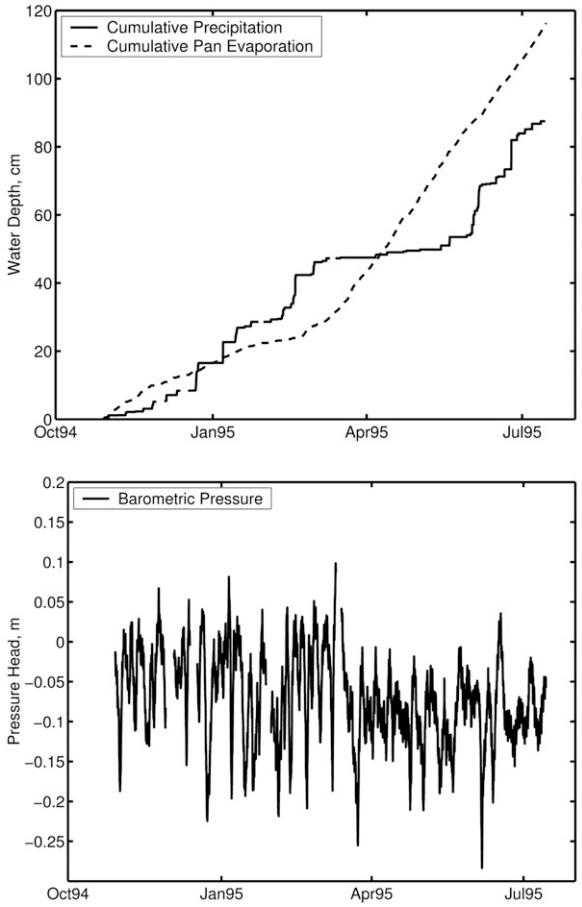

FIG. 3. Plots of observed cumulative precipitation and cumulative pan evaporation (top), and barometric pressure (bottom) between 29 Oct. 1994 and 14 July 1995 at Well Cluster FSB-120, Savannah River Site, SC.

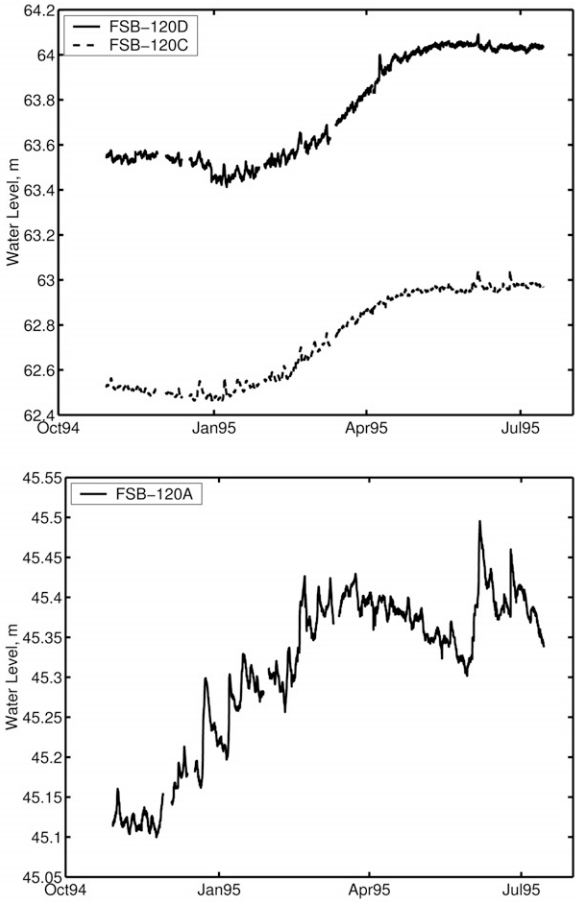

FIG. 4. Plots of observed water levels in FSB-120D (unconfined aquifer) and FSB-120C (semiconfined aquifer) (top), and FSB-120A (confined aquifer) (bottom) between 29 Oct. 1994 and 14 July 1995. Ground surface elevation is 85 m.

ments. This provided the ability to resolve differences in water levels to 0.12 cm (Bruns, 2000).

Estimates of potential evapotranspiration were obtained using pan evaporation data from a weather station located at Sandhill Plantation, Elgin, SC (34.13°N, 80.87°W). This station was selected because the soils and vegetation surrounding the weather station are similar to conditions at the study site. Potential evapotranspiration was also estimated using a program developed by Allen et al. (1998) with weather data from the Sandhill Plantation site and the Penman method (Penman, 1948).

The theoretical Earth tide potential was estimated using TSoft (Royal Observatory of Belgium, 2006; Van Camp and Vauterin. 2005), a software package that provides times series of theoretical Earth-tide potentials for user-selected locations and time periods. Mathematical computations were obtained using MATLAB (Mathworks, 2006).

Results and Discussion

Figure 3 presents cumulative precipitation (top) and barometric pressure (bottom) at the FSB-120 well cluster. Figure 4 presents borehole water levels in three boreholes (corresponding to the unconfined, semiconfined, and confined aquifers) at the well cluster. The data span an 8-mo period from 29 Oct. 1994 through 14 July 1995. A few brief intervals with data loss resulting from equipment failures can be observed in the figure. The unconfined and semiconfined aquifers show a slow increase in water levels following winter precipitation. Figure 4 also shows the lack of a corresponding increase in the confined aquifer, as well as a rapid response to precipitation events.

Figure 5 (top) shows a scatterplot between barometric pressure changes, $\triangle B$, and FSB-120A water-level changes, $\triangle W$, with an estimated barometric efficiency of α = 6%. The calculated differences were taken between successive observations, $\triangle t$ = 10 min. Also shown (bottom) is the scatterplot between precipitation plus barometric pressure changes, P + $\triangle B$ vs. FSB-120A total head changes, $\triangle H_b$. The estimated (instantaneous) loading efficiency is the slope of this line, equivalent to β = 91% or α = 9%.

The lagged aquifer response to loading changes is illustrated in Fig. 6. The initial response was approximately β = 95%, falling to approximately β = 83% within 30 min. This lagged response could be due, in part, to the time required for water levels to equilibrate between the borehole and the aquifer. An additional cause may be a time delay for water to equilibrate between isolated and active porosity within the aquifer. The instantaneous estimate, β = 91%, lies within the range of observations for the lagged response.

Well performance tests are routinely conducted at the Savannah River Site to evaluate response times for water-level changes in monitoring wells. A slug test was performed on Well

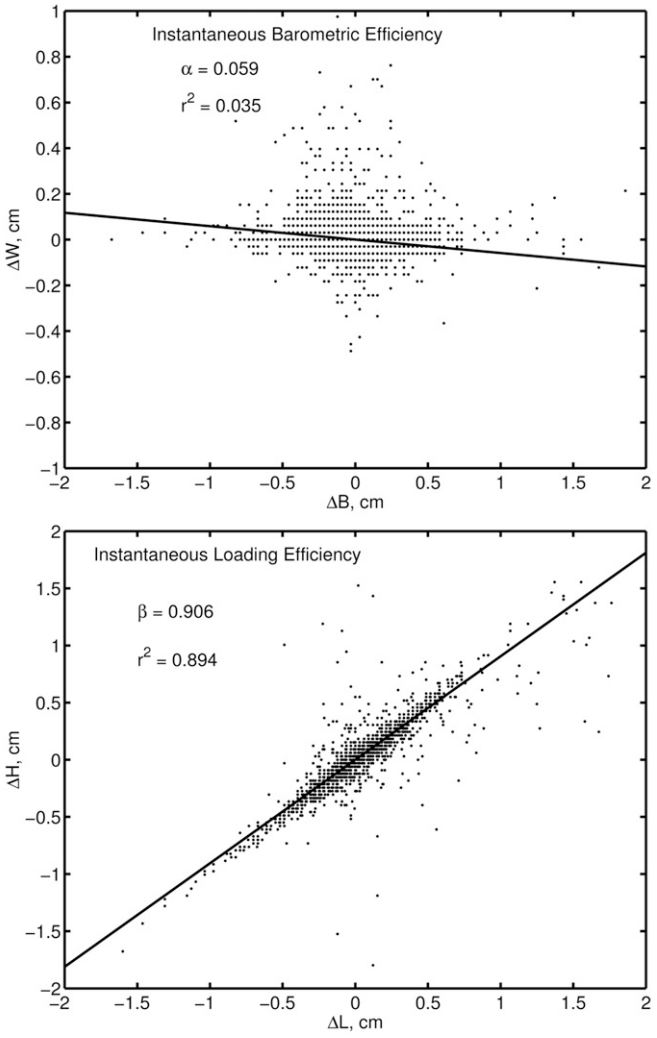

FIG. 5. Scatter diagrams between barometric pressure changes, $\triangle B$, and FSB-120A water levels, $\triangle W$, (top), and between precipitation plus barometric pressure changes, $\triangle L$, and borehole head changes, $\triangle H$ (bottom). Data differences are calculated between successive observations collected at 10-min intervals.

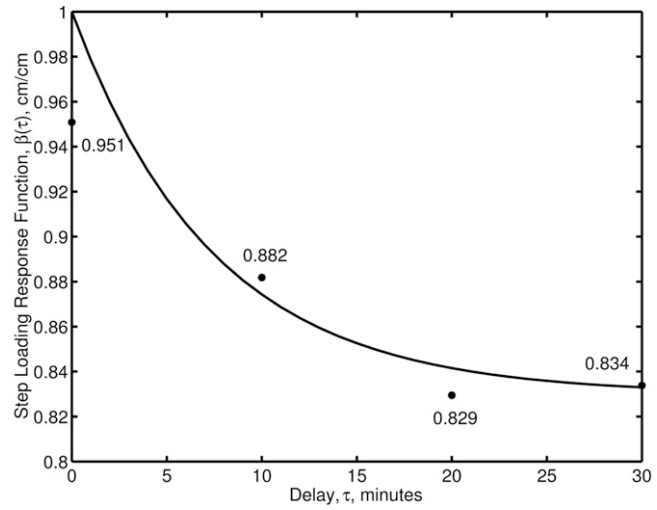

FIG. 6. Step loading response function between borehole head changes and precipitation plus barometric pressure changes. Also shown is the slug test response assuming a final barometric efficiency of $\beta = 0.82$. The function reaches a stable value within approximately 30 min, indicating that equilibration between the borehole and the aquifer is rapid but not instantaneous.

FSB-120A by Westinghouse Environmental and Geotechnical Services, Inc. (Columbia, SC) on 3 December 1990 (Dan Wells, personal communication). The resulting water level response was fitted using (Bouwer and Rice, 1976; Bouwer, 1989)

$$h = h_o \exp(-m\tau) \quad [16]$$

where h is the observed water level change as a function of lag time, τ, h_o = 110 cm is the water level immediately after the slug volume was added, and m = 0.135 is the exponential slope coefficient. The slope coefficient corresponds to a 90% reduction in water levels after approximately 17 min. The slope coefficient was also used to estimate a local hydraulic conductivity of 20 cm per day, which is lower than the regional estimate of 860 cm per day. Also shown in Fig. 6 is the slug test response, using an initial value of $\beta_o = 100\%$, the estimated exponential recession coefficient, and an ultimate loading efficiency of $\beta_\infty = 83\%$, so that $\beta(\tau) = \beta_o - (\beta_o - \beta_\infty) \exp(-m\tau)$.

Figure 7 illustrates the calculated influence of the theoretical Earth-tide potential (top) and the calculated Earth-tide influence (bottom), the magnitudes of which are provided in Table 2. The two are markedly different. The calculated influence is a statistical estimate of the most likely periodic functions that remove the maximum amount of water-level variability. Reasons for the

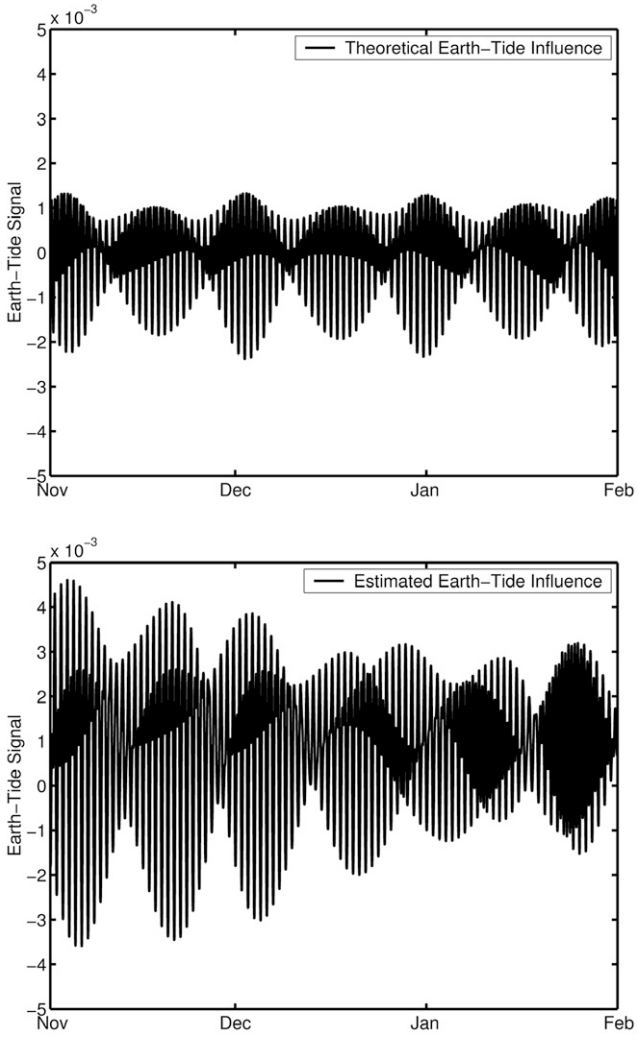

FIG. 7. Influence of theoretical Earth-tide potential (top) and calculated Earth tides (bottom) on water levels.

TABLE 2. Tidal cycles used to remove periodic aquifer water level fluctuations (Melchior, 1983). Semidiurnal periods are one-half the diurnal period. Also shown are the estimated magnitudes, $(a_i^2 + b_i^2)^{1/2}$, and phase lags, $a\tan(b_i/a_i)$, of the tidal influence on water levels at Well FSB-120A, Savannah River Site, SC.

	Diurnal components				Semidiurnal components		
Component	Period	Amplitude	Phase lag		Period	Amplitude	Phase lag
	h	cm	rad		h	cm	rad
M1	24.8412	0.0004	1.3730	M2	12.4206	0.0083	1.5405
O1	25.8193	0.0016	1.4484	O2	12.9097	0.0012	2.5288
P1	24.0659	0.0044	2.7274	P2	12.0329	0.0063	2.1172
K1	23.9345	0.0050	4.5474	K2	11.9672	0.0041	5.0800
N1	25.3167	0.0004	2.1081	N2	12.6583	0.0014	2.0098

lack of similarity can be ascribed to the differential response of aquifers to Earth-tide loading due to variations in aquifer material properties (Rojstaczer and Agnew, 1989).

Knowing the loading efficiency allows us to remove the effects of barometric pressure changes and Earth tides from the water-level record. Figure 8 (top) shows the original water-level record along with the interpreted load for two cases. The first case neglects delays in loading and uses the theoretical Earth tide, whereas the second case accounts for loading delays and uses the lagged Earth-tide signals. The second case has a substantially smoother appearance, and short-term transients are less pronounced. Figure 8 (bottom) also presents the cumulative water export that represents the effects of water storage changes once measured precipitation has been removed.

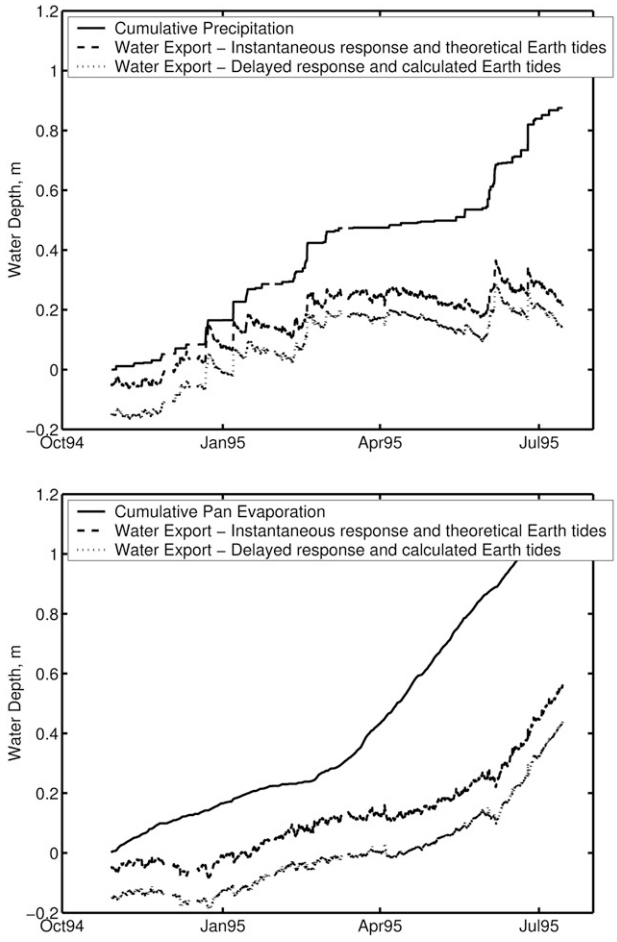

FIG. 8. Cumulative precipitation and water storage estimated using two methods: (a) instantaneous loading response plus theoretical Earth-tide removal, and (b) delayed loading response plus calculated Earth-tide removal (top), and pan evaporation with water exports using the same two methods (bottom).

Water exports increased slowly during the late fall, with an increasing rate during the winter due to increased precipitation. The spring season saw a flattening of water export due to minimal precipitation during this period, presumably from a decrease in evapotranspiration as the soil water content decreased. The water exports increased, however, as precipitation increased during late spring. Slight declines during late November through early December are perplexing but may result from lateral surface or groundwater migration.

Total precipitation for the period at the well cluster was 87.5 cm, compared to an export of 65.3 cm, implying a net water storage increase of 22.2 cm. Precipitation and measured pan evaporation for the same period at the nearby weather station at Sandhill Plantation, were 91.5 and 115.7 cm, respectively, corresponding to a net change of –24.2 cm. (The Penman equation was used to provide an independent estimate of evapotranspiration loss of 125.3 cm, which is consistent with the pan loss.) The discrepancy between the estimated export using water-level data and weather data (42.0 cm) could be due to evapotranspiration rates that are lower than pan evaporation, or net lateral groundwater flux at the site. Using a pan factor of 70% yields an actual evapotranspiration of 81 cm, which is closer to the export value of 65.3 cm but is still substantially different. It is not currently possible to distinguish between these two alternatives without additional data.

Figure 9 presents a more focused examination for the period 3–18 June 1995, which included an individual precipitation event. There was a rapid response in water levels as a result of precipitation (top). There was also an apparent overestimation of the actual rainfall from the groundwater observations for the larger rain event, which may have resulted from gauge undercatch or possibly significant spatial rainfall variation over the site. The water export remained steady after the precipitation event, and pan evaporation rates were similar to the water export rate (bottom).

Nondaily fluctuations attributed to Earth tides are observed in the series corrected using the theoretical Earth tide potential but are absent in the series estimated using calculated Earth tides. Both series show a lack of a daily periodicity, even though a daily signal was not removed from the calculated series. A loss of pressure due to vertical leakage could explain the observed response. To evaluate this possibility, Fig. 10 presents concomitant water levels during the 3–18 June 1995 period in all three units. It shows a similarity in response between the confined (FSB-120A, upper) and overlying semiconfined (FSB-120C, middle) aquifers.

Although there was a clear response to precipitation loading in the semiconfined aquifer, this was likely due to direct loading on the aquifer itself rather than upward leakage because (i) the intervening aquitard is known to have very low hydraulic conductivity and (ii) the lag time between the two responses is small—vertical leakage between the units would result in a substantial lag time. The response in the unconfined aquifer (Fig. 10, FSB-120D, lower) is likely due to upward vertical leakage from the semiconfined below it. The rise and fall of the water

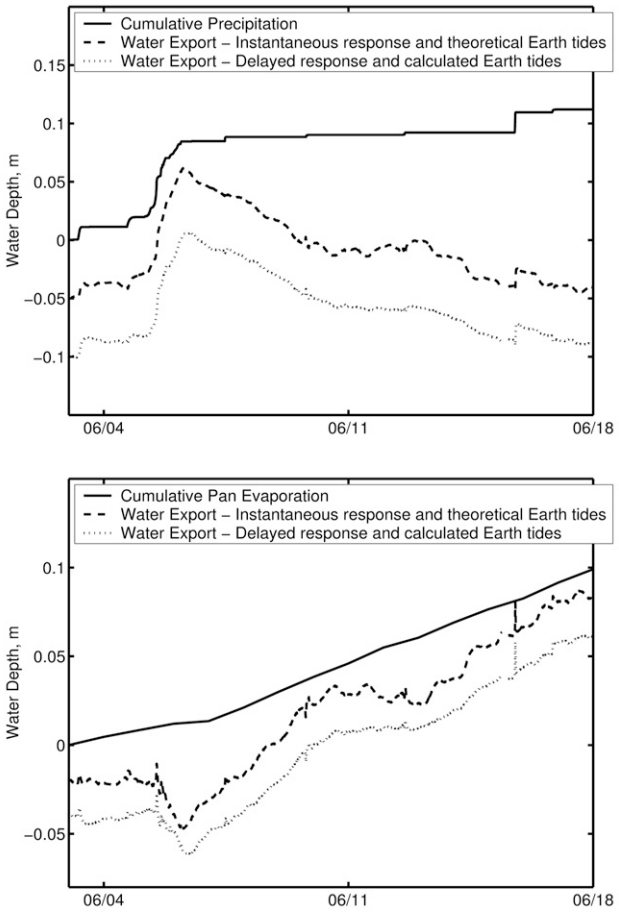

FIG. 9. Detail of a precipitation event (3–18 June 1995) showing cumulative precipitation and water storage estimated using two methods: (a) instantaneous loading response and theoretical Earth tides, and (b) delayed loading response with synthetic Earth-tide removal (top), and pan evaporation with water exports using the same two methods (bottom).

table without any evident precipitation event during 11–15 June might be speculated as a brief period of decreased water export due, perhaps, to the passage of a water-table wave originating from higher on the slope.

Finally, a speculative estimate of the surface area of influence associated with monitoring well FSB-120A can be obtained by assuming a one-dimensional, uniform load across the site and a conical influence zone above the aquifer. The monitored surface area is $A = \pi r^2$ where $r = z\tan\gamma$ is the radius of surface influence, and where z = 51.6 m is the aquifer depth, and $\gamma = 60°$ is the conical angle of influence. The resulting area calculated using this method is approximately A = 2.5 ha. The actual response to point loads requires the monitoring of water levels associated with application of loads over a range of distances.

Conclusions

Water levels in confined aquifers often fluctuate in response to external events. At the Savannah River Site, the Gordon aquifer responded weakly to barometric pressure changes (instantaneous barometric efficiency ∼6%) but strongly to precipitation events (instantaneous loading efficiency ∼91%). This can be explained by noting that surface loading at this site is borne

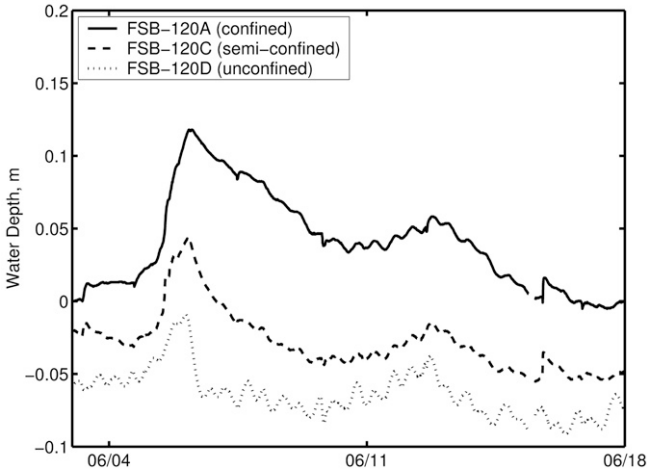

FIG. 10. Detail of a precipitation event (3–18 June 1995) showing water levels in three hydrogeologic units, FSB-120A (upper plot), FSB-120C (middle plot), and FSB-120D (lower plot). Curves have been offset to allow simultaneous comparison on the same scale.

largely by aquifer fluids instead of the aquifer skeleton due to the lack of consolidation in these recent coastal sediments.

The response to loading at this site is not instantaneous; a complete equilibration between the borehole and surrounding aquifer required 30 min. This is consistent with well performance data that show a similar response. The accuracy associated with assuming an instantaneous response affects the resulting water-balance calculation. Minimizing borehole storage by isolating the monitoring interval using packers would reduce this effect.

Our study shows that at least one confined, sedimentary aquifer at the Savannah River Site may be suitable for use as a geologic weighing lysimeter. The accuracy of the geologic weighing lysimeter for determining water budgets is limited by (i) the inability to accurately estimate components of the budget, such as evapotranspiration and lateral surface and subsurface flows (which means that they can be reliably estimated only up to the limit of remaining sources of uncertainty in the water budget), (ii) the presence of natural and anthropogenic signals, including barometric, Earth tides, and local water withdrawals, and (iii) the hydraulic isolation of the geologic unit, both horizontally and vertically. Accounting for water budget uncertainties—as well as demonstrating the isolation of the target geologic unit—will require additional characterization at this site. Additional monitoring that would assist interpretation at this site includes the use of replicated experimental measurements over two or more vertically separated, confined aquifers.

The suitability of other geologic units to provide meaningful estimates of soil water budgets rests on both their geologic origin and their proximity to other disturbances. Consolidated geologic units with poor compressibility (β < 10% and a > 90%) are not likely to provide accurate water storage estimates because of their small loading efficiency. An additional requirement is that lateral fluxes within and above the target geologic unit are constant, or can be measured, so that flow dynamics apart from the loading affect can be characterized. Also, geologic units with substantial anthropogenic water-level manipulation, such as pumping or independent loading, may mask natural processes. Hence, the target geologic unit should be poorly consolidated and isolated from other geologic units and anthropogenic sources.

While the geologic weighing lysimeter provides an estimate of water storage, it does not specifically isolate the location of the stored water. Whether the water is stored on or within aboveground vegetation, on the ground surface, within or below the root zone, or within the surficial aquifer is beyond the capacity of this approach to discriminate. The only claim that can be made is that changes in total load above the confined aquifer are occurring and can be estimated.

Acknowledgments

Data collection was funded by a grant from the USDOE, Westinghouse Savannah River Corporation through the Education, Research, and Development Association of Georgia Universities titled "Investigation of water level variations in ground-water monitoring wells, and the potential impact on regulatory compliance in the ground-water monitoring program at the Savannah River Site," WSRC 94075EQ, with technical support provided by John Reed and Dan Wells of the Savannah River Site. The manuscript was substantially improved by review comments from W.E. Bardsley and G. van der Kamp.

References

Aadland, R.K. 1993. Hydrogeological synthesis for the Savannah River Site region. WSRC-TR-93-102. Westinghouse Savannah River Company, Aiken, SC.

Aadland, R.K., J.A. Gelici, and P.A. Thayer. 1995. Hydrogeologic framework of west-central South Carolina. Report 5. SC Dep. Nat. Resour., Water Resour. Div., Columbia, SC.

Allen, R.G., L.S. Pereira, D. Raes, and M. Smith. 1998. Crop evapotranspiration: Guidelines for computing crop water requirements. FAO Irrigation and Drainage Paper No. 56. FAO, Rome, Italy.

Bardsley, W.E., and D.I. Campbell. 1994. A new method for measuring near-surface moisture budgets in hydrological systems. J. Hydrol. 154:245–254.

Bardsley, W.E., and D.I. Campbell. 1995. Water loading: A neglected factor in the analysis of piezometric time series from confined aquifers. J. Hydrol. 34:89–93 (NZ).

Bardsley, W.E., and D.I. Campbell. 2000. Natural geological weighing lysimeters: Calibration tools for satellite and ground surface gravity monitoring of subsurface water mass change. Nat. Resour. Res. 9:147–156.

Barr, A.G., G. van der Kamp, R. Schmidt, and T.A. Black. 2000. Monitoring the moisture balance of a boreal aspen forest using a deep groundwater piezometer. Agric. For. Meteorol. 102(1):13–24.

Bouwer, H. 1989. The Bouwer and Rice slug test: An update. Ground Water 27(3):304–309.

Bouwer, H., and R.C. Rice. 1976. A slug test method for determining hydraulic conductivity of unconfined aquifers with completely or partially penetrating wells. Water Resour. Res. 12(3):423–428.

Bruns, A.C. 2000. Investigation of ground water level fluctuations at the Savannah River Site. Master's thesis. Univ. of Georgia, Athens.

Davis, D.R., and T.C. Rasmussen. 1993. A comparison of linear regression with Clark's method for estimating barometric efficiency of confined aquifers. Water Resour. Res. 29:1849–1854.

Furbish, D.A. 1991. The response of water level in a well to a time series of atmospheric loading under confined conditions. Water Resour. Res. 27(4):557–568.

Jacob, C.E. 1940. On the flow of water in an elastic artesian aquifer. Trans. Am. Geophys. Union 21:574–586.

Mathworks. 2006. MATLAB, Version 6.1. Available at www.mathworks.com (verified 17 May 2006). Mathworks, Inc., Natick, MA.

McCuen, R.H. 2004. Hydrologic analysis and design. 3rd ed. Prentice Hall, Upper Saddle River, NJ.

Melchior, P.J. 1983. The tides of the planet Earth. Pergamon Press, New York.

Pascal, B. 1973. The physical treatises of Pascal. Octagon Books, New York.

Penman, H.L. 1948. Natural evaporation from open water, bare soil, and grass. Proc. R. Soc. London, Ser. A 193:120–145.

Rasmussen, T.C., and L.A. Crawford. 1997. Identifying and removing barometric pressure effects in confined and unconfined aquifers. Ground Water 35(3):502–511.

Rasmussen, T.C., K.G. Haborak, and M.H. Young. 2003. Estimating aquifer hydraulic properties using sinusoidal pumping at the Savannah River Site, South Carolina, USA. Hydrogeol. J. 11:466–482.

Rogers, V.A. 1990, Soil survey of Savannah River Plant area, parts of Aiken, Barnwell, and Allendale Counties, South Carolina. USDA, Soil Cons. Serv., Washington, DC.

Rojstaczer, S., and D.C. Agnew. 1989. The influence of formation material properties on the response of water levels in wells to Earth tides and atmospheric loading. J. Geophys. Resear. B 94:12403–12411.

Royal Observatory of Belgium. 2006. TSoft, ver. 2.0.14. Available at www.astro.oma.be/SEISMO/TSOFT/tsoft.html (verified 8 Feb. 2007). Royal Observatory of Belgium, Brussels.

Sophocleous, M., E. Bardsley, and J. Healey. 2006. A rainfall loading response recorded at 300 meters depth: Implications for geological weighing lysimeters. J. Hydrol. 319(1–4):237–244.

Spane, F.A. 2002. Considering barometric pressure in groundwater flow investigations. Water Resour. Res. 38(6):1078.

Spane, F.A., and R.B. Mercer. 1985. HEADCO: A program for converting observed water levels and pressure measurements to formation pressure and standard hydraulic head. RHO-BW-ST-71P. Basalt Waste Isolation Project, Rockwell Hanford Operations, Richland, WA.

Timms, W.A., and R.I. Acworth. 2005. Propagation of pressure change through thick clay sequences: An example from Liverpool Plains, NSW, Australia. Hydrogeol. J. 13(5–6):858–870.

Van Camp, M., and P. Vauterin. 2005. TSoft: Graphical and interactive software for the analysis of time series and Earth tides. Comput. Geosci. 31(5):631–640.

van der Kamp, G., and R. Maathuis. 1991. Annual fluctuations of groundwater levels as a result of loading by surface moisture. J. Hydrol. 127(1–4):137–152.

van der Kamp, G., and R. Schmidt. 1997. Monitoring of total soil moisture on a scale of hectares using groundwater piezometers. Geophys. Res. Lett. 24(6):719–722.